Nano Energy 90 (2021) 106614

Contents lists available at ScienceDirect

Nano Energy

journal homepage: www.elsevier.com/locate/nanoen

Anti-freezing organohydrogel triboelectric nanogenerator toward highly efficient and flexible human-machine interaction at − 30 °C

Zhenyu Xu [a,b], Fenghua Zhou [c], Huizhen Yan [a,b], Guorong Gao [a,b,*], Huijing Li [a,b], Rui Li [a], Tao Chen [a,b,*]

[a] Key Laboratory of Marine Materials and Related Technologies, Zhejiang Key Laboratory of Marine Materials and Protective Technologies, Ningbo Institute of Materials Technology and Engineering, Chinese Academy of Sciences, Zhongguan West Road 1219, 315201 Ningbo, China
[b] School of Chemical Sciences, University of Chinese Academy of Sciences, Beijing 100049, China
[c] UNISOC Technologies Co., Ltd., Shanghai 201203, China

ARTICLE INFO

Keywords:
Anti-freezing
Organohydrogel
Triboelectric nanogenerator
Sensor
Keyboard

ABSTRACT

Human-machine interaction is crucial for mobile communications, Internet of Things, intelligent medical care, and intelligent robots. There is an increasing interest to develop the next generation of flexible human-machine interactive devices based on stretchable ionic conductive polymer gels. However, due to the nature of polymer gels, the devices turn brittle and the ionic conductivity dramatically drops at subzero temperatures, thus restricted their applicable temperature range. Herein, anti-freezing organohydrogels consist of polyacrylamides/nano-clays networks absorbed with ethylene glycol (EG)/water were designed. The anti-freezing binary solution provides excellent properties for organohydrogels at − 30 °C, including tensile modulus of 29.2 kPa, an ultimate tensile strain of 700%, the ionic conductivity of 1.5×10^{-3} S m^{-1}, transparency of 91%, and rapid self-healing. The flexible organohydrogels electrodes were assembled with elastomers to prepare triboelectric nanogenerators (TENGs), which were further attached on fingers to develop human-machine interactive keyboards. The voltage signals produced by the keyboards in contact with many surfaces were collected, coded, and interpreted as letters and punctuations, then displayed on a monitor. We demonstrated typing by using the self-powered flexible keyboard at − 30 °C. This work may benefit the development of anti-freezing soft materials, self-powered sensors, and wearable human-machine interaction communication device systems.

1. Introduction

Human-machine interaction is essential for the Internet of Things, humanoid robots and intelligent medical apparatus, and instruments [1–3]. Most of the present human-machine interactive devices, such as the most common keyboards, mouses, and touch panels are made from rigid or fragile materials, and not suitable for wearable use. There is a great need to develop the next generation of human-machine interactive devices [4–7], which should be soft with modulus be comparable to that of human skin (~10^7 Pa) [8], be stretchable to adapt to the body movement [9], and be preferably self-powering to avoid the using of heavy batteries and tedious charging steps [10].

Ionic conductive polymer gels, including hydrogels [11], organohydrogels [12] and ionic liquid gels [13] are chemically or physically cross-linked three dimensional polymer networks containing liquids and mobile ions. These soft gels have adjustable mechanical properties [14–17] and electrical conductivity [18,19], have been widely researched to develop soft and stretchable sensors [11,20–25] and integrated into wearable human-machine interactive devices [5,6,26]. For example, Yu et al. reported an ionogel composed of fluorine-rich poly (ionic liquid) and ionic liquid that showed adjustable underwater conductivity and stretchability [27]. It was made into a resistive sensor, attached to a prosthetic finger, and worked as a wearable keyboard by coding the signals of finger bending into the Morse code [27]. Lee et al. reported a kind of flexible human-machine interactive communicator made from hydrogel triboelectric nanogenerators (TENGs) [28]. The voltage signals were coded and interpreted to the 26 alphabets. TENGs convert mechanical energy into electrical energy via coupling triboelectric effect and electrostatic induction effects [10,29–32], are attractive devices as mechanical energy harvester [33–36] and

* Corresponding authors at: Key Laboratory of Marine Materials and Related Technologies, Zhejiang Key Laboratory of Marine Materials and Protective Technologies, Ningbo Institute of Materials Technology and Engineering, Chinese Academy of Sciences, Zhongguan West Road 1219, 315201 Ningbo, China.
E-mail addresses: gaogr@nimte.ac.cn (G. Gao), tao.chen@nimte.ac.cn (T. Chen).

https://doi.org/10.1016/j.nanoen.2021.106614
Received 7 July 2021; Received in revised form 27 September 2021; Accepted 6 October 2021
Available online 12 October 2021

self-powered sensors [37–39] for healthcare monitoring or human-machine interaction sense. However, hydrogels freeze at subzero temperatures, resulting in loss of flexibility and stretchability and a significant decrease in ionic conductivity.

In nature, many plants and animals can survive extremely cold weather by preventing the formation of ice crystals in cells. These creatures accumulated cryoprotectants, such as urea [40] and glucose [41], in tissues, thus depressed the freezing point of bodily fluids. Inspired by this principle, some cryoprotectants, including $CaCl_2$ [42], glycerin [43], glycerol [44,45], and ethylene glycol (EG) [46,47] have been used as additives to synthesize the anti-freezing gels. EG is widely used in industrial cooling systems to prevent water from freezing. In EG/water binary solution, EG and water form molecular clusters, breaking the hydrogen bond network of water, and preventing the formation of ice crystals [48,49]. The presence of EG leads to reduced saturated vapor pressure of the binary solution, thus results in decreased freezing point [50,51].

Herein, we report anti-freezing and flexible human-machine interactive devices based on organohydrogel TENG. The TENG consists of two pieces of VHB™ 4905 transparent elastomer sandwiched with a piece of ionic conductive organohydrogel that is connected to a metal electrode (Fig. 1a). The organohydrogel is prepared through solvent replacement of a hydrogel in EG/water binary solvent and the hydrogel is synthesized through in-situ polymerization of the monomer acrylamide (AAm) in an aqueous solution of nano-clays. Thus, both hydrogel (Fig. 1b) and organohydrogel (Fig. 1c) were composed of the physically cross-linked polymer networks, which are polyacrylamide (PAAm) chains adsorbed on nano-clays, and absorbed with corresponding liquids. The mobile ions are sodium ions from clays. The TENG generated a pulse voltage signal during contact to and separate from a surface (Fig. 1d). We attached five TENGs on five fingers, collected and converted the five channel signals to binary codes by a demo board, then intepreted the binary codes to letters and punctuations for display on a monitor (Fig. 1e). At − 30 °C, the organohydrogel TENG showed a modulus of 101 kPa, ultimate tensile strain of 539%, open-circuit voltage (V_{oc}) of 72 V, and power density of 57.3 mW m^{-2} with Nylon as the contact material. We demonstrated typing by using the wearable keyboard at − 30 °C. Our strategy may benefit the development of anti-freezing organohydrogel TENG toward highly efficient and flexible human-machine interaction at − 30 °C.

2. Material and methods

2.1. Materials

Synthetic nano-clays (Laponite XLG) were purchased from BYK Additives & Instruments. Acrylamide (AAm) and ethylene glycol (EG) were purchased from the Sinopharm Chemical Reagent Co., Ltd. Ammonium persulfate (APS) and N, N, N′, N′-Tetramethylethylenediamine (TEMED) was purchased from Aladdin Chemistry Co., Ltd. VHB™ 4905 was obtained from 3 M Corporation. All chemicals were used as received. Deionized water was used in all experiments.

2.2. Preparation of hydrogel

Nano-clays (0.381 g, 0.5 mmol) were dissolved in water (10 mL) and stirred for 2 h. Then, AAm (2.1324 g, 30 mmol) was added to the solution, followed by stirring for another 2 h. Next, APS (0.0034 g, 0.015 mmol) and TEMED (5 μL, 0.055 mmol) were added and stirred for 10 min. The final solution was poured into a mold composed of two plate glasses and a silicone frame with an inner size of 60 mm × 60 mm × 1 mm. The transparent hydrogel was obtained after

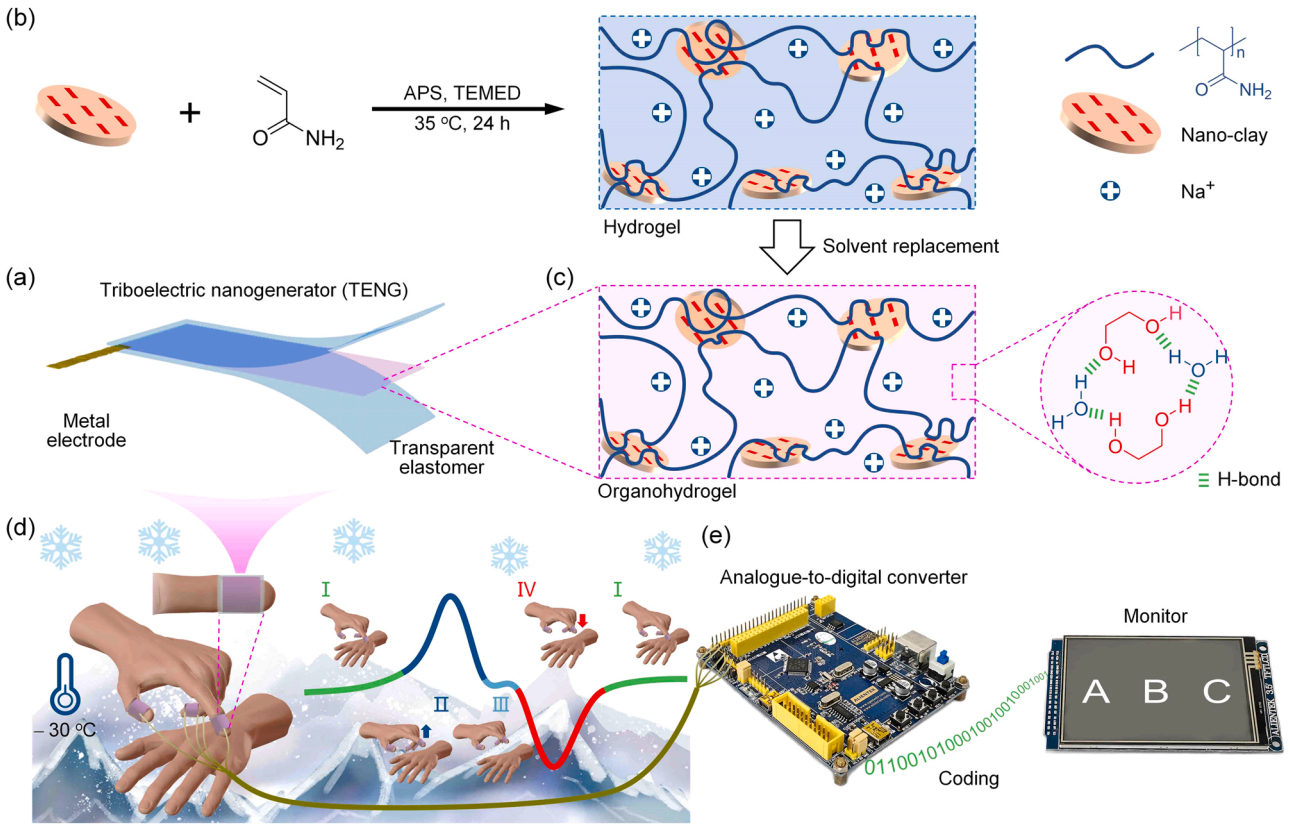

Fig. 1. Designing of organohydrogel TENG toward the human-machine interactive keyboard. Schematic illustration of (a) the architecture of TENG, (b) the synthesis process of hydrogel, (c) the structure of organohydrogel, (d) five TENGs on five fingers generate pulse voltage signals as the fingers contact to and separate from skin, and (e) the voltage signals were collected, converted into binary codes, interpreted into letters and output to a monitor.

polymerizing at 35 °C for 24 h.

2.3. Preparation of organohydrogel

A hydrogel sample (size, 30 mm × 30 mm × 1 mm) was soaked in 60 mL of EG/water binary solution (EG: water = 5: 1, *vol*: *vol*) for 6 h to get an organohydrogel. The obtained organohydrogel maintained the same size.

2.4. Preparation of self-healing samples

The hydrogels or organohydrogels were cut into two sections, followed by joining the cross-sections together. These assemblies were sealed in polyethylene films, then stored at a determined temperature for a determined time.

2.5. Preparation of organohydrogel TENG

Organohydrogel TENG was prepared by sandwiching a piece of organohydrogel (size, 30 mm × 30 mm × 1 mm) between two pieces of VHB™ 4905 elastomer (thickness, 500 μm), with a copper foil electrode connected to organohydrogel. Hydrogel TENG was obtained by the same method.

2.6. Preparation of finger-cot keyboard

Five TENGs were attached to five fingers, like five finger-cots. Each TENG was connected to an independent signal capture circuit, then connected to an independent channel in a Mini STM32 demo board (Guangzhou Xingyi Electronic Technology Co., Ltd). The demo board convert the electric signals into digital signals, coded and interpreted as alphabet through its "brain", the microcontroller unit.

2.7. Measurement of phase transition points

The phase transition points of gel samples were measured by a differential scanning calorimeter (NETZSCH DSC 214) from − 145 to 40 °C with a heating rate of 3 °C min^{-1}.

2.8. Mechanical tests

The tensile tests were conducted on a Zwick Roell Z1.0 universal material testing machine. The strip samples with a size of 25 mm × 8 mm × 1 mm with a crosshead distance of 10 mm were stretched at a constant speed of 50 mm min^{-1}. Before testing, the samples were stored at 25 or − 30 °C for at least 12 h. The modulus was determined as the slope of the stress-strain curve in the strain range of 0–50%. The strain was calculated as $(l-l_0)/l_0 \times 100\%$, where l was the length and l_0 was the initial length. The dynamic mechanical analysis was performed on a DMAQ800 analyzer (TA, America) with a temperature sweep in the range of − 30–25 °C at a constant strain of 20 μm and frequency of 10 Hz.

2.9. Measurement of conductivity

The conductivity was studied by alternating current impedance spectroscopy technique and conducted on a Chenhua CHI660E electrochemical workstation. A gel sample with a size of 25 mm × 8 mm × 1 mm was sandwiched between two copper electrodes with the same area. Sinusoidal voltage waves with an amplitude of 0.01 V and frequency range from 0.1 to 10^5 Hz were applied to the sample. The resulted real (Z′) and imaginary parts (Z″) of impedance at different frequencies were recorded as a Nyquist plot.

2.10. Measurement of output characteristics

The output performances (V_{oc}, I_{sc}, Q_{sc}, and power density) of TENGs were recorded by a Keithley 6514 electrometer, and that at subzero temperatures were measured in a freezer.

3. Results and discussion

Organohydrogels were anti-freezing in comparison with the hydrogels. Differential scanning calorimetry (DSC) curves were recorded from − 145 to 40 °C (Fig. 2a). A weak endothermic peak appeared at − 118.2 °C for organohydrogel, which is the glass transition temperature of the EG/water binary solution [52], and no freezing point was observed in DSC curve, indicating EG/water mixtures in organohydrogels maintained liquid until − 118.2 °C. In contrast, a huge peak was observed at − 0.8 °C for hydrogel, which is freezing point of water in hydrogel.

Organohydrogels showed tensile fracture strain of 1124% at 25 °C, and 700% at − 30 °C, and have the same modulus of 29.2 kPa at the two temperatures (Fig. 2b). At − 30 °C, the organohydrogel hung softly off the tweezers as if it was 25 °C (Fig. 2b). As a comparison, the hydrogels showed fracture strain of 2148% and modulus of 48 kPa at 25 °C (Fig. S1), but were too brittle to conduct tensile tests at − 30 °C (Fig. S2). We have tried to immerse as-prepared hydrogels in EG/water solutions with different ratios (EG: water = 1: 1, 2: 1, 3: 1, 4: 1 and 5: 1, *vol*: *vol*) for 6 h to prepare organohydrogels. The organohydrogels prepared from the 5: 1 EG/water solution showed minimum volume swelling (Fig. S3a) and maximum breaking strength of 126 kPa at room temperature (Fig. S3b), as the polyacrylamide network tends to absorb water rather than EG. So, the organohydrogels used in this work were prepared in the 5: 1 EG/water solution.

The mechanical properties loss of organohydrogels at − 30 °C can be attributed to the decreased polymer activity at low temperatures. As temperature decreases, the relaxation time of polymer chain increases, which results in reduced chain flexibility and mechanical property of materials. Dynamic mechanical (DMA) tests were conducted to further evaluate the influence of temperature on mechanical properties of organohydrogels and hydrogels. In Fig. S4, as the temperature decreases from 25 to − 30 °C, the storage modulus (G′) of organohydrogel slightly increased from 60 to 90 kPa, in contrast, the G′ of hydrogel sharply increased from 1.9×10^2 to 1.1×10^7 kPa. These results indicate that the changes of mechanical property for organohydrogels were dominated by thermal motion of polymers, while that for hydrogels were dominated by water frozen from 25 to − 30 °C.

Mechanical properties of organohydrogels are partially self-healing (Fig. 2c). The cut-then-joined organohydrogels were respectively stored at 25 and − 30 °C for determined times before the tensile tests. Organohydrogels healed at 25 °C for 48 and 24 h recovered the fracture strain to 705% and 462%, respectively, while that healed at − 30 °C for 24 showed a fracture strain of 337%, with a healing efficiency of 48.1%. The organohydrogels are cross-linked through physical adsorption between polyacrylamides and nano-clays (Fig. 1c), and no chemical cross-linking agent was added during material synthesis. The physical adsorption is attributed to hydrogen bonds between $–NH_2$ in polyacrylamide chains and oxygen atoms in laponite clays [5]. In cut-then-joined samples, the polymer chains diffused across the joint faces, leading to new cross-linking points and self-healing. The healing efficiency increased by enhancing temperature and prolonging storing time (Fig. 2c), indicating that the accelerated polymer thermal motion and prolonged-time are beneficial for the generation of new cross-linking points.

Compared to hydrogels, the conductivity of organohydrogels is less affected by temperature. Fig. 2d and e show the Nyquist plots of organohydrogels and hydrogels. The conductivity (σ) could be calculated from the plot by $\sigma = d/RS$, where d is the thickness, S is the area of organohydrogel, and R is equal to the point value at which the plot

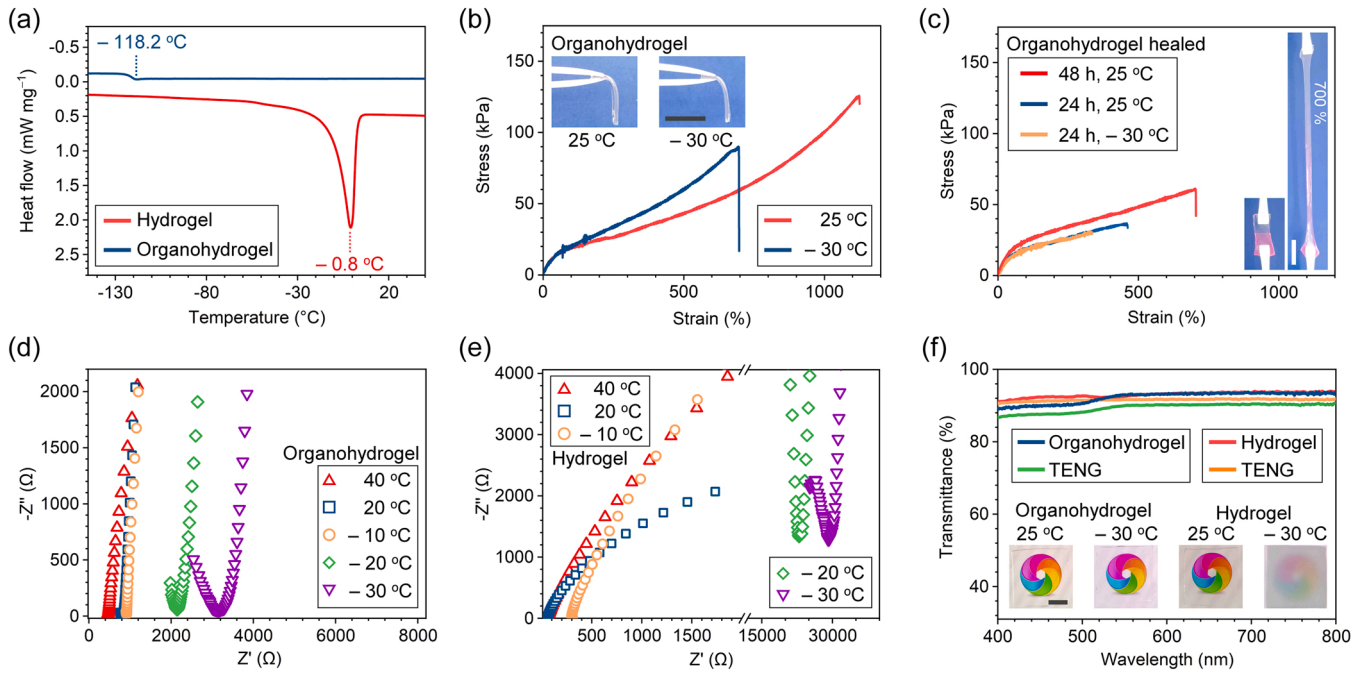

Fig. 2. Anti-freezing properties of organohydrogels. (a) DSC curves of hydrogel and organohydrogel. (b) Photos and tensile stress-strain curves of organohydrogels at 25 and − 30 °C. (c) Tensile stress-strain curves of organohydrogels self-healed at 25 and − 30 °C for determined times. Inserted photos show an organohydrogel self-healed at 25 °C for 48 h was stretched to 700%. Nyquist plots of (d) organohydrogels and (e) hydrogels at determined temperatures. (f) Transmittance spectra of organohydrogel, hydrogel and corresponding TENGs. Inserted photos reflected the transparency at 25 and − 30 °C. Scale bars, 1 cm.

intersects the Z′ axis. In the case where there is no intersection point, the R is determined as the Z′ value corresponding to the lowest point of the plot (Fig. 2e). The conductivities of organohydrogels decreased by temperature drop, were $1 \times 10^{-2} \pm 4.2 \times 10^{-4}$ (standard deviation calculated from $n = 5$) and $1.5 \times 10^{-3} \pm 1.1 \times 10^{-4}$ S m^{-1} at 40 and − 30 °C, respectively (Fig. 2d). In sharp contrast, the conductivities of hydrogels decreased greatly by temperature decreasing (Fig. 2e), were $9.6 \times 10^{-2} \pm 4.6 \times 10^{-3}$ S m^{-1} at 40 °C and $1.4 \times 10^{-4} \pm 5 \times 10^{-6}$ S m^{-1} at − 30 °C, respectively, indicating the freezing of hydrogels severely impeded the migration of inner ions. The organohydrogels are rapid self-healing in conductivity. At 20 and − 30 °C, the cut-then-joined organohydrogels showed very similar conductivity to that of original samples (Fig. S5).

Organohydrogels are highly transparent in the visible light region (wavelength from 400 to 800 nm, Fig. 2f). The average transparency is 91.5% and 89.4% for organohydrogel and corresponding TENG, while is 93% and 92.2% for hydrogel and corresponding TENG. The colored patterns behind organohydrogels are visible at 25 and − 30 °C (Fig. 2f, inserted photos), but are hardly seen for that behind the opaque hydrogel at − 30 °C. These results suggest that solvent displacement didn't induce perceptible phase change of polymers, and there are no ice crystals generated in organohydrogels at − 30 °C.

The principle of alternating current produced by a TENG is contact electrification and electrostatic induction (Fig. 3a) [10,32,53–57]. When a contact material, such as a Nylon plate used in Fig. 3, encounters the TENG, contact electrification occurs due to the difference in electron affinity between the two materials (Fig. 3a, step I). Once separate, the static (negative) charges in the insulating elastomer of TENG attract the opposite (positive) ions and repel the same charge (negative) ions, thereby inducing the directed migration of ions in organohydrogel (Fig. 3a, step II). Meanwhile, electrons flow from the metal electrode to the ground due to electrostatic equilibrium, thus the electric current is detected (Fig. 3a, step II). A new electrostatic equilibrium is established until all static charges in the elastomer were screened (Fig. 3a, step III). Once the contact material is approaching back to the elastomer, electrons flow back from the ground due to electrostatic induction, and electric current in the reverse direction is detected (Fig. 3a, step IV).

To measure the output performance, including open-circuit voltage (V_{oc}), short-circuit current (I_{sc}) and short-circuit charge quantity (Q_{sc}), a reciprocating motor with a Nylon plate at the top was used to cyclically tap the organohydrogel TENG (size, 3 cm × 3 cm) at a frequency of 2.5 Hz. At 40, 20, − 10, − 20 and − 30 °C, the V_{oc} is 83.9, 86, 79, 76.3 and 72 V, respectively (Fig. 3b); I_{sc} is 0.73, 0.76, 0.58, 0.56 and 0.54 μA, respectively (Fig. 3c); and Q_{sc} is 26.9, 28, 26, 25.6 and 24.2 nC (Fig. 3d). At 40 and 20 °C, organohydrogel TENGs have similar output performance. From 20 to − 30 °C, the V_{oc}, I_{sc} and Q_{sc} slightly decreased by decreasing of temperature. At − 30 °C, organohydrogel TENG showed remarkable electricity generation capability, and could light up 14 blue LEDs at − 30 °C (Movie. S1). The output power density (P) of TENG on an external resistance (R) was obtained by measuring the output voltage (U) and output current (I), and calculated as $P = UI$. The U increased while I decreased as R increased from 10^6 to 5×10^9 Ω (Fig. 3e and f). The maximum P of organohydrogel TENG was 75.4 mW m^{-2} at 20 °C and R of 10^8 Ω (Fig. 3e), and was 57.3 mW m^{-2} at − 30 °C and the same 10^8 Ω (Fig. 3f), which is 76% that of the former. Conversely, the hydrogel TENGs lost their function as generators below − 20 °C. As shown in Fig. S6, the V_{oc}, I_{sc} and Q_{sc} of hydrogel TENG was 88.8 V, 74.5 μA and 28.6 nC at 20 °C, respectively, but was decreased to 0.8 V, 0.05 μA and 2.3 nC at − 20 °C, and was further decreased to indistinguishable at − 30 °C.

The output characteristics of TENGs at various temperatures are in accordance with the variation of conductivity of organohydrogels and hydrogels. Since EG is more viscous than water, the introduction of EG to gels leads to increased migration resistance of ions, which further results in a lower conductivity of organohydrogels (Fig. 2d) in comparison to that of corresponding hydrogels at 20 °C (Fig. 2e). At − 30 °C, the hydrogels are frozen (Fig. 2a and Fig. S2), accordingly, the ionic carriers are trapped in ice crystals and lost mobility, therefore, electrostatic induction induced ions migration in TENG (step II in Fig. 3a) may not occurrence, i.e., a hydrogel TENG lost its function as a generator. Nylon was selected because it gives the highest V_{oc} in comparison with other materials including PET, PTFE, PDMS and silicone rubber

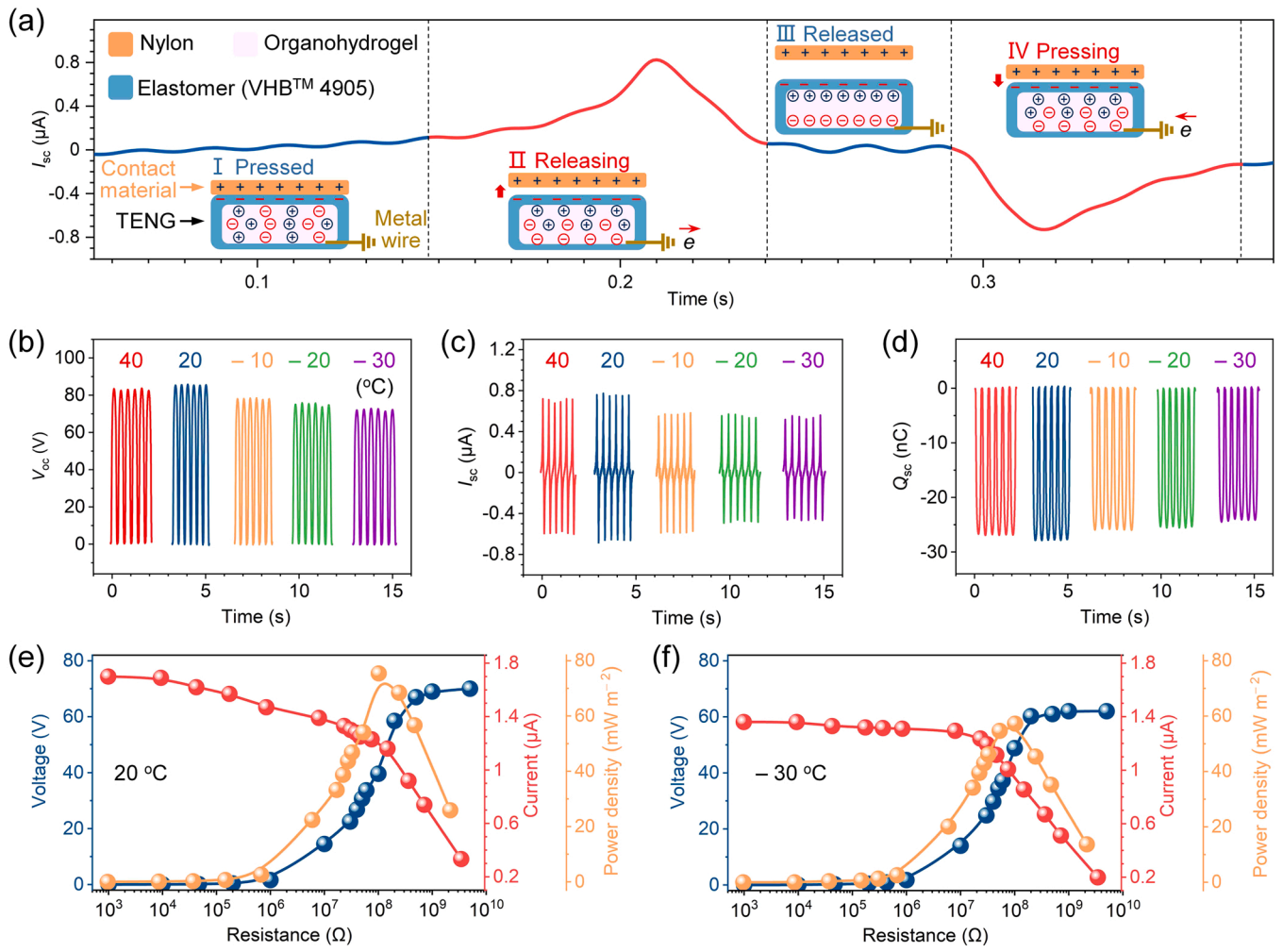

Fig. 3. Working mechanism and output characteristics of organohydrogel TENGs. (a) The short-circuit current (I_{sc}) recorded in a contact-separation cycle as a TENG was tapped by a Nylon plate, and schemes show the working mechanism of TENG. The (b) open-circuit voltage (V_{oc}), (c) I_{sc} and (d) short-circuit charge quantity (Q_{sc}) of TENGs. Variation of voltage, current and power density with external resistances at (e) 20 °C and (f) − 30 °C.

(Fig. S7).

Organohydrogel TENGs are stretchable at − 30 °C. The TENG has a modulus of 101 kPa and fracture strain of 539% at − 30 °C, and that of 78.8 kPa and 710% at 25 °C (Fig. S8). The stretchability of TENG is restricted by the fracture of VHB™ elastomer. Fig. 4a shows a TENG was stretched to a strain of 500% at − 30 °C. Fig. 4b shows the V_{oc} of a TENG (20 mm × 10 mm) when it was stretched to 50%, 100%, 150%, 200%, 300%, 400%, 500% then recovered at − 30 °C. In each step, it was tapped by a Nylon plate (50 mm × 100 mm) at 2.5 Hz. The V_{oc} first increased from 32.6 to 42.3 V, as strain changed from 0% to 300%. It further decreased to 29.8 V at a stain of 400% and 16.2 V at strain of 500%, then recovered to 30 V as the TENG retracted to its initial size. These results indicate the TENGs are suitable to be used as components of stretchable human-machine interactive devices or self-supply powers at subzero temperatures.

The variation of V_{oc} by stretching of TENG is affected by the synergistic effects of surface area and resistance changes. Assuming that the volume of the TENG is unchanged during deformation. When the TENG is stretched to λ (= strain+1) times its initial length, its width and thickness are reduced by a factor of $\lambda^{1/2}$, simultaneously, and the area is increased by a factor of $\lambda^{3/2}$ [11]. Meanwhile, the resistance of organohydrogel increased by a factor of λ^2, theoretically [6]. As the triboelectric area increasing, the amount of charges increased in contact electrification, results in a bigger V_{oc} [53]. On the other hand, the decrease of conductivity of organohydrogel (Fig. S9) leads to weaker electrostatic induction, results in a smaller V_{oc}. The overall effect is V_{oc} first increased then decreased in strain from 0% to 500%.

Organohydrogel TENGs are self-healing, stable and durable at − 30 °C. Fig. 4c shows the V_{oc} of a TENG (area, 30 mm × 30 mm) was constant at 72 V when it was unbroken and cut-then-joined, indicating it could rapidly regain output characteristics after suffering from mechanical injury. Fig. 4d shows the V_{oc} was kept in 72 V when a TENG was tapped for 3000 cycles. In Fig. 4e, the V_{oc} was almost unchanged for a TENG stored at − 30 °C for 30 days.

The excellent stability and durability of TENGs are mainly attributed to the bonding performance of VHB™ elastomer. As shown in Fig. 4a, the up and down VHB™ layers are bonded at the edge, and the organohydrogel is sealed in TENG. Evaporation from organohydrogel is prevented. Organohydrogel TENGs have an average weight retention ratio of 97% after storing at 25 °C in an atmospheric environment (Fig. S10). Fig. S11 shows the V_{oc} is constant at 90 V before and after the TENG storing at 25 °C for 30 days. Although several anti-freezing gels prepared by adding inorganic salt, organic solvents, ionic liquids have been reported to prepare TENGs [58–65]. There are few gel materials based TENGs that are anti-freezing, ultra-stretchable, transparent, self-healing and have high output voltage at the same time (Table S1).

We harvested the electrical energy to power the wearable device at − 30 °C. As shown in the equivalent circuit (Fig. 5a), the output of a TENG could be rectified to charge a capacitance, and then used to power electron devices. Fig. 5b showed the 4.7, 10 and 47 μF capacitances

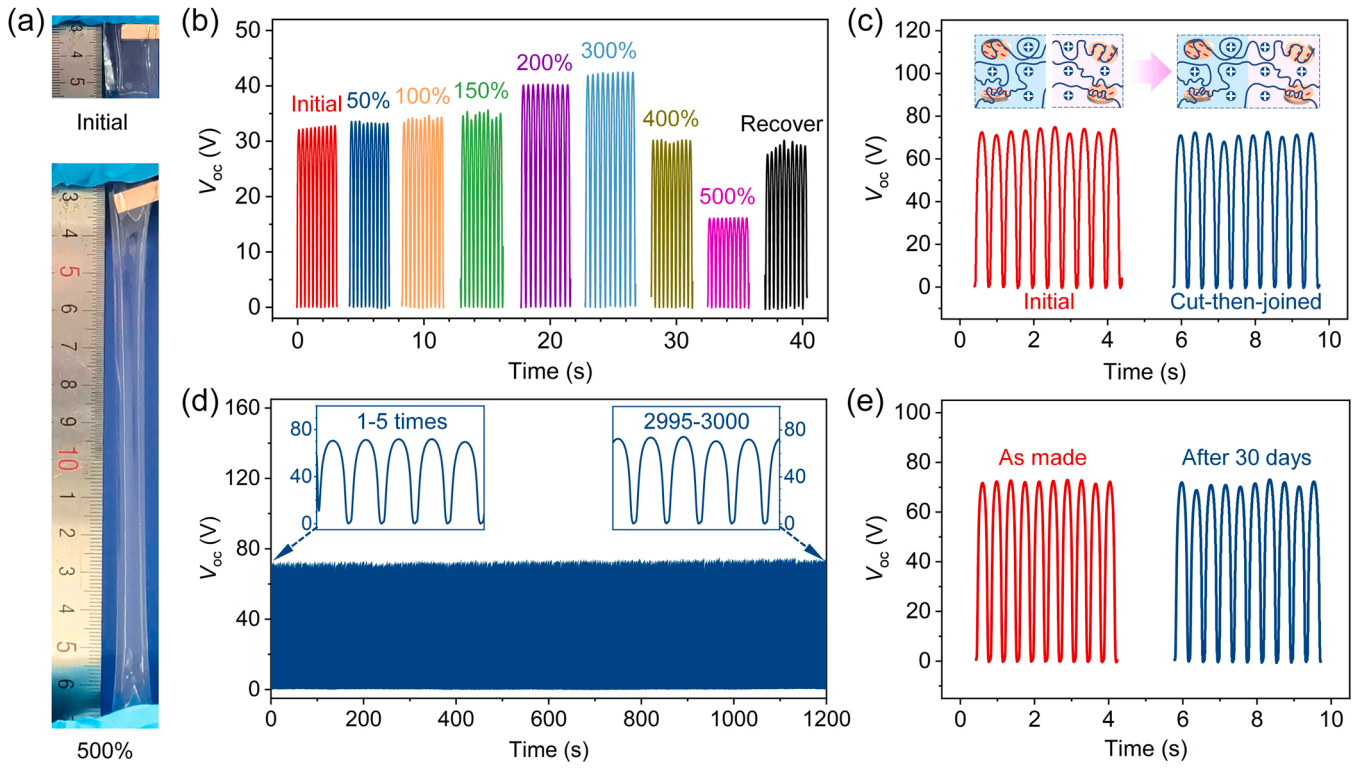

Fig. 4. Stretchability, self-healing, stability and durability of organohydrogel TENGs at − 30 °C. (a) Photos show a TENG was stretched to a strain of 500%. (b) The V_{oc} of a TENG (initial area 1 × 2 cm^2) under varied tensile strains. (c) The V_{oc} of a TENG (area 3 × 3 cm^2) before and after cut-then-joining. (d) The V_{oc} of a TENG in 3000 tapping cycles. (e) The V_{oc} of a TENG before and after storing for 30 days.

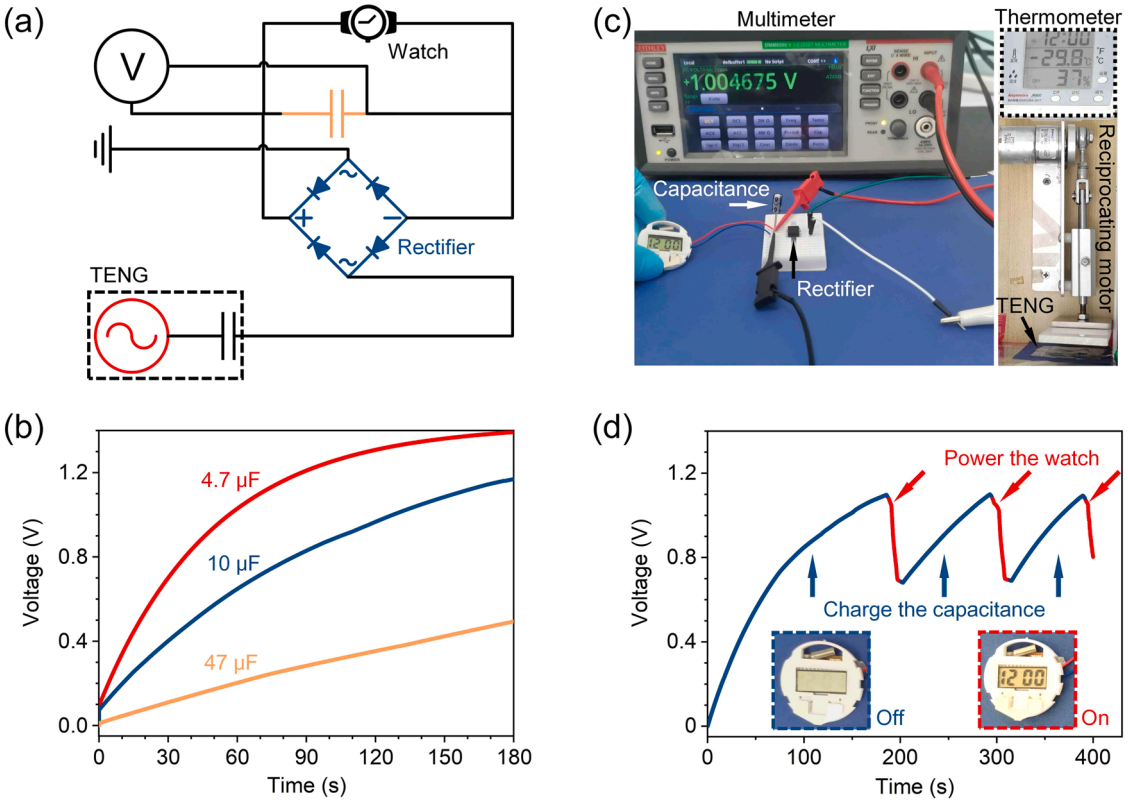

Fig. 5. Energy harvesting at − 30 °C. (a) The equivalent circuit of charging a capacitance to power a watch. (b) Charging behaviors for capacitances. (c) Photos show a capacitance charged by a TENG is powering a watch. (d) Voltage varied by time when a 10 μF capacitor was charged by a TENG and used to power the watch.

reached 1.4, 1.2 and 0.5 V in 180 s, respectively, as a TENG (30 mm × 30 mm) in Fig. 5c was cyclically tapped at a frequency of 2.5 Hz. A 10 μF capacitance was chosen to power an electron watch (Fig. 5c). The capacitance was first charged by taping the TENG for 180 s, enabling powering watch for 7 s (Fig. 5d and Movie S2), then was charged again by taping for 90 s and enabling powering watch for another 7 s, the later cycle is repeatable. These results suggest the TENG has a potential function to power the flexible human-machine interactive devices at subzero temperatures.

A flexible human-machine interactive system was developed based on the organohydrogel TENGs. The TENGs were attached on five fingers of a hand with VHB^{TM} elastomers come into contact with the skin. According to the working mechanism of TENG (Fig. 3a), a voltage signal generates as a finger contact to and separated from a substrate. If we define the occurring of voltage signal (finger tapping) as "1" and the absence of voltage (not tapping) as "0" (Fig. 6a), there are 2^5-1 variations for 5 fingers tapping individually or simultaneously, and each tapping gesture could be expressed by a five-bit binary digit, from 00001 to 11111. We defined that the bits from left to right as the results of little, ring, middle, index and thumb fingers (Fig. 6a), respectively, and interpreted each binary digit as a letter, punctuation or function key (Fig. 6b). So, the five TENGs act as a keyboard.

The circuit diagram in Fig. 6c illustrates the signal evolution in the human-machine interactive system. A signal acquisition circuit was designed to detect the voltage from TENGs. The voltage pulse generated from a TENG will make an instantaneous change of constant voltage on the connected field-effect transistors (FETs) (Movie S3). The constant voltage was applied by the demo board. Then, the microcontroller unit (MCU) in demo board distinguished the tapping or no tapping of the fingers according to the voltage waveform of the transistor, and generated the five-bit binary digits. Finally, the characters corresponding to the binary digits were displayed on a monitor. At − 30 °C, significant voltages generated from gentle touches to cotton fabric (0.7 V), skin (1.3 V) and rubber gloves (2 V) (Fig. 6d).

We demonstrated typing by using the human-machine interactive system at − 30 °C. The letters "CNITECH" were written by tapping the

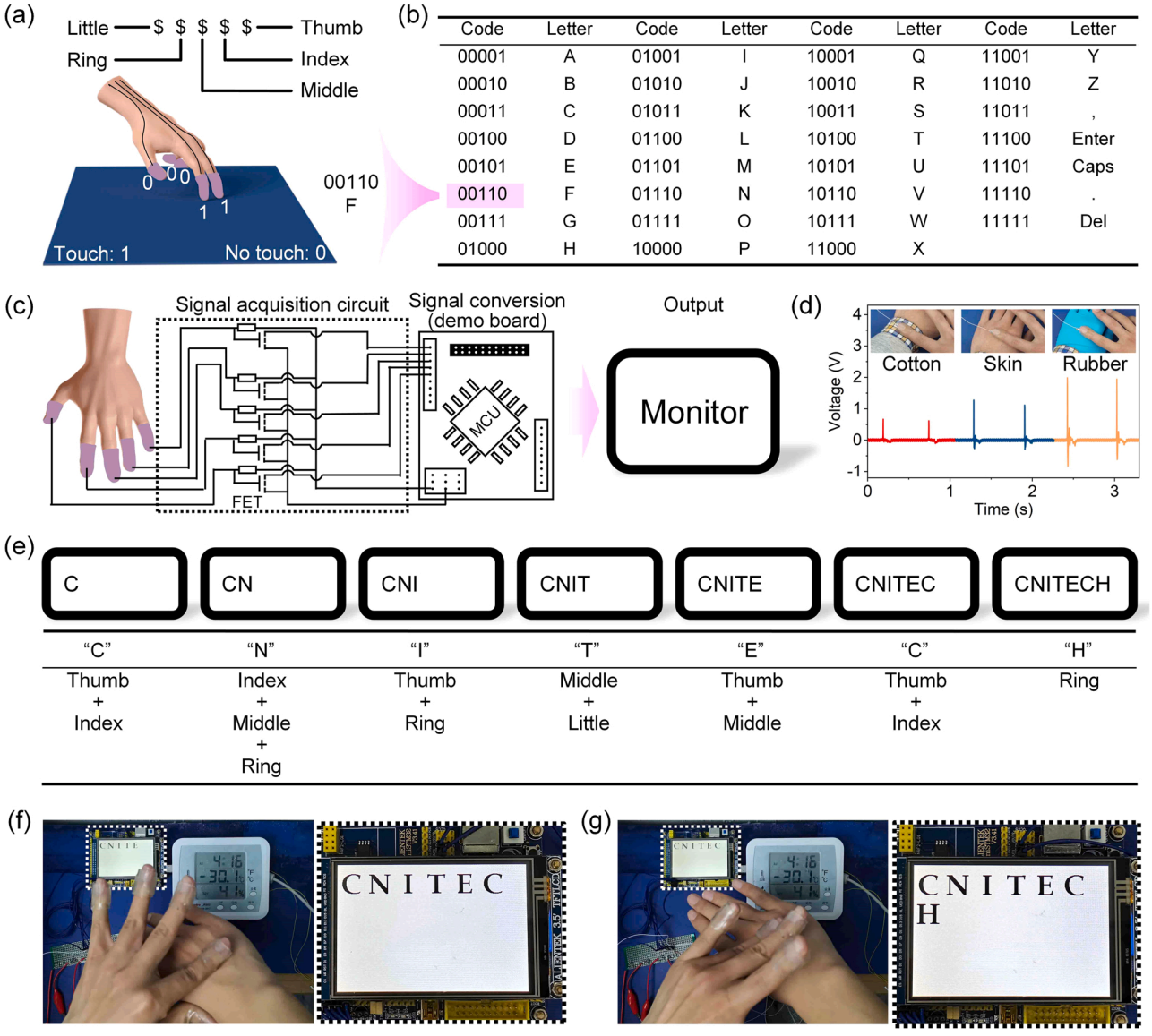

Code	Letter	Code	Letter	Code	Letter	Code	Letter
00001	A	01001	I	10001	Q	11001	Y
00010	B	01010	J	10010	R	11010	Z
00011	C	01011	K	10011	S	11011	,
00100	D	01100	L	10100	T	11100	Enter
00101	E	01101	M	10101	U	11101	Caps
00110	F	01110	N	10110	V	11110	.
00111	G	01111	O	10111	W	11111	Del
01000	H	10000	P	11000	X		

Fig. 6. Anti-freezing and flexible human-machine interactive system based on organohydrogel TENGs. (a) Schematic illustration of the definition of "0" and "1". (b) A table lists the letters, punctuations and function keys corresponding to 31 five-bit binary digits. (c) A detailed diagram of the self-powered sensor, signal acquisition circuit, signal processing board and displayer. (d) Voltages generated from gentle touch of keyboard to cotton fabric, skin and rubber gloves. (e) Schemes illustration of the combination of fingers when typing the abbreviation CNITECH of Ningbo Institute of Industrial Technology, Chinese Academy of Sciences. Photos of typing the (f) letters "C" and (g) "H" at − 30 °C.

fingers following the combinations in Fig. 6e. For examples, the "C" was input by simultaneously touching thumb and index to skin (Fig. 6f), and the "H" was written by touching the ring finger to skin (Fig. 6g and Movie S4). Furthermore, the wearable keyboards worked when fingers bending (Movie S5), in which scenario the TENGs were stretched to certain extents. The response time of the organohydrogel TENG is 2 ms (Fig. S12). The MCU treated the signals within 1 s as simultaneous pressing to facilitate the novice-operators.

Previously, Lee et al. [28] have reported a kind of wearable keyboard based on hydrogel TENGs. Our organohydrogel TENG keyboards have two advantages in comparison with the former devices. The organohydrogel TENG keyboards are anti-freezing that could work at minus 30 degrees, while hydrogel TENG froze at subzero temperature. We use a five-bit binary digit to denote a letter, and the "1" and "0" in the binary digit respectively denote "press" and "not press" of a specific finger. Such coding helps the typist operate the keyboard. In contrast, the former coding used a decimal number to represent a letter, thus the typist had to work out which fingers to press simultaneously to get the decimal number.

4. Conclusions

A type of anti-freezing ionic conductive organohydrogels composed of polyacrylamides/nano-clays physical networks and the freezing tolerant ethylene glycol (EG)/water binary solutions was designed, with Na^+ from nano-clays as mobile ions. By tuning the EG/water ratio, organohydrogels with a modulus of 29.2 kPa, stretchability of 700% and conductivity of 1.5×10^{-3} S m^{-1} at − 30 °C were obtained. The organohydrogels showed rapid self-healing in conductivity, and partial self-healing in mechanics at − 30 °C. Triboelectric nanogenerators (TENGs) with the organohydrogel as electrostatic induction layer and VHB™ elastomer as triboelectric layer were designed. The TENGs were mechanically compliant with a modulus of 101 kPa and stretchability of 539%, and showed V_{oc} of 72 V, I_{sc} of 0.54 μA, Q_{sc} of 24 nC and maximum output power density of 57.3 mW m^{-2} with Nylon as contact material at − 30 °C. Furthermore, the stretchable TENGs were stable, durable and self-healable, and demonstrated to harvest energy to power wearable watch at − 30 °C. A human-machine interactive system was developed by using the TENGs as self-powered sensors. The voltage signals from TENGs on five fingers were coded, then interpreted as an alphabet to output. The organohydrogels, corresponding TENGs and human-machine interactive systems show exiting potentials in the field of wearable self-powered sensors, soft robotics and unobtrusive surveillance communicators at subzero temperatures.

CRediT authorship contribution statement

Zhenyu Xu: Conceptualization, Methodology, Investigation, Writing – original draft, Visualization. **Fenghua Zhou**: Conceptualization, Methodology, Software, Resources. **Huizhen Yan**: Investigation. **Guorong Gao**: Conceptualization, Methodology, Writing – review & editing, Project administration, Funding acquisition. **Huijing Li**: Investigation. **Rui Li**: Investigation. **Tao Chen**: Conceptualization, Methodology, Writing – review & editing, Supervision, Funding acquisition.

Declaration of Competing Interest

The authors declare no competing financial interest.

Acknowledgements

This work was supported financially by National Natural Science Foundation of China (51773215), Key Research Program of Frontier Sciences, Chinese Academy of Sciences (QYZDB-SSW-SLH036), Zhejiang Provincial Natural Science Foundation of China (LY21E030013), Ningbo Scientific and Technological Innovation 2025 Major Project (2018B10057, 2020Z022), Ningbo Natural Science Foundation (202003N4359), the Sino-German Mobility Program (M-0424), and K.C. Wong Education Foundation (GJTD-2019-13).

Appendix A. Supporting information

Supplementary data associated with this article can be found in the online version at doi:10.1016/j.nanoen.2021.106614.

References

[1] X. Yu, Z. Xie, Y. Yu, J. Lee, A. Vazquez-Guardado, H. Luan, J. Ruban, X. Ning, A. Akhtar, D. Li, B. Ji, Y. Liu, R. Sun, J. Cao, Q. Huo, Y. Zhong, C. Lee, S. Kim, P. Gutruf, C. Zhang, Y. Xue, Q. Guo, A. Chempakasseril, P. Tian, W. Lu, J. Jeong, Y. Yu, J. Cornman, C. Tan, B. Kim, K. Lee, X. Feng, Y. Huang, J.A. Rogers, Skin-integrated wireless haptic interfaces for virtual and augmented reality, Nature 575 (2019) 473–479.
[2] S.N. Flesher, J.E. Downey, J.M. Weiss, C.L. Hughes, A.J. Herrera, E.C. Tyler-Kabara, M.L. Boninger, J.L. Collinger, R.A. Gaunt, A brain-computer interface that evokes tactile sensations improves robotic arm control, Science 372 (2021) 831–836.
[3] C.H. Yang, Z.G. Suo, Hydrogel ionotronics, Nat. Rev. Mater. 3 (2018) 125–142.
[4] L. Zhang, J. He, Y.S. Liao, X.T. Zeng, N.X. Qiu, Y. Liang, P. Xiao, T. Chen, A self-protective, reproducible textile sensor with high performance towards human-machine interactions, J. Mater. Chem. A 7 (2019) 26631–26640.
[5] G. Gao, F. Yang, F. Zhou, J. He, W. Lu, P. Xiao, H. Yan, C. Pan, T. Chen, Z.L. Wang, Bioinspired self-healing human-machine interactive touch pad with pressure-sensitive adhesiveness on targeted substrates, Adv. Mater. 32 (2020), e2004290.
[6] C.C. Kim, H.H. Lee, K.H. Oh, J.Y. Sun, Highly stretchable, transparent ionic touch panel, Science 353 (2016) 682–687.
[7] J.X. Wang, M.F. Lin, S. Park, P.S. Lee, Deformable conductors for human-machine interface, Mater. Today 21 (2018) 508–526.
[8] D. Rus, M.T. Tolley, Design, fabrication and control of soft robots, Nature 521 (2015) 467–475.
[9] K. Sim, Z. Rao, F. Ershad, C. Yu, Rubbery electronics fully made of stretchable elastomeric electronic materials, Adv. Mater. 32 (2020), e1902417.
[10] F.R. Fan, W. Tang, Z.L. Wang, Flexible nanogenerators for energy harvesting and self-powered electronics, Adv. Mater. 28 (2016) 4283–4305.
[11] J.Y. Sun, C. Keplinger, G.M. Whitesides, Z. Suo, Ionic skin, Adv. Mater. 26 (2014) 7608–7614.
[12] J. Lee, M.W.M. Tan, K. Parida, G. Thangavel, S.A. Park, T. Park, P.S. Lee, Water-processable, stretchable, self-healable, thermally stable, and transparent ionic conductors for actuators and sensors, Adv. Mater. 32 (2020), e1906679.
[13] Y. Ren, Z. Liu, G. Jin, M. Yang, Y. Shao, W. Li, Y. Wu, L. Liu, F. Yan, Electric-field-induced gradient ionogels for highly sensitive, broad-range-response, and freeze/heat-resistant ionic fingers, Adv. Mater. 33 (2021), e2008486.
[14] C. Liu, N. Morimoto, L. Jiang, S. Kawahara, T. Noritomi, H. Yokoyama, K. Mayumi, K. Ito, Tough hydrogels with rapid self-reinforcement, Science 372 (2021) 1078–1081.
[15] M. Hua, S. Wu, Y. Ma, Y. Zhao, Z. Chen, I. Frenkel, J. Strzalka, H. Zhou, X. Zhu, X. He, Strong tough hydrogels via the synergy of freeze-casting and salting out, Nature 590 (2021) 594–599.
[16] J.Y. Sun, X. Zhao, W.R. Illeperuma, O. Chaudhuri, K.H. Oh, D.J. Mooney, J. J. Vlassak, Z. Suo, Highly stretchable and tough hydrogels, Nature 489 (2012) 133–136.
[17] G. Gao, G. Du, Y. Sun, J. Fu, Self-healable, tough, and ultrastretchable nanocomposite hydrogels based on reversible polyacrylamide/montmorillonite adsorption, ACS Appl. Mater. Interfaces 7 (2015) 5029–5037.
[18] T.B.H. Schroeder, A. Guha, A. Lamoureux, G. VanRenterghem, D. Sept, M. Shtein, J. Yang, M. Mayer, An electric-eel-inspired soft power source from stacked hydrogels, Nature 552 (2017) 214–218.
[19] C. Keplinger, J.Y. Sun, C.C. Foo, P. Rothemund, G.M. Whitesides, Z. Suo, Stretchable, transparent, ionic conductors, Science 341 (2013) 984–987.
[20] Z. Lei, Q. Wang, S. Sun, W. Zhu, P. Wu, A bioinspired mineral hydrogel as a self-healable, mechanically adaptable ionic skin for highly sensitive pressure sensing, Adv. Mater. 29 (2017), 1700321.
[21] P. Cai, C. Wan, L. Pan, N. Matsuhisa, K. He, Z. Cui, W. Zhang, C. Li, J. Wang, J. Yu, M. Wang, Y. Jiang, G. Chen, X. Chen, Locally coupled electromechanical interfaces based on cytoadhesion-inspired hybrids to identify muscular excitation-contraction signatures, Nat. Commun. 11 (2020) 2183.
[22] I. You, D.G. Mackanic, N. Matsuhisa, J. Kang, J. Kwon, L. Beker, J. Mun, W. Suh, T. Y. Kim, J.B. Tok, Z. Bao, U. Jeong, Artificial multimodal receptors based on ion relaxation dynamics, Science 370 (2020) 961–965.
[23] J. Li, D.J. Mooney, Designing hydrogels for controlled drug delivery, Nat. Rev. Mater. 1 (2016) 16071.
[24] J. Liu, S. Lin, X. Liu, Z. Qin, Y. Yang, J. Zang, X. Zhao, Fatigue-resistant adhesion of hydrogels, Nat. Commun. 11 (2020) 1071.
[25] J. Li, A.D. Celiz, J. Yang, Q. Yang, I. Wamala, W. Whyte, B.R. Seo, N.V. Vasilyev, J. J. Vlassak, Z. Suo, D.J. Mooney, Tough adhesives for diverse wet surfaces, Science 357 (2017) 378–381.
[26] Z. Lei, W. Zhu, X. Zhang, X. Wang, P. Wu, Bio-inspired ionic skin for theranostics, Adv. Funct. Mater. 31 (2020), 2008020.

[27] Z. Yu, P. Wu, Underwater communication and optical camouflage ionogels, Adv. Mater. 33 (2021), e2008479.
[28] Y. Lee, S.H. Cha, Y.W. Kim, D. Choi, J.Y. Sun, Transparent and attachable ionic communicators based on self-cleanable triboelectric nanogenerators, Nat. Commun. 9 (2018) 1804.
[29] Z.L. Wang, Triboelectric nanogenerators as new energy technology for self-powered systems and as active mechanical and chemical sensors, ACS Nano 7 (2013) 9533–9557.
[30] J.W. Zhong, Q.Z. Zhong, F.R. Fan, Y. Zhang, S.H. Wang, B. Hu, Z.L. Wang, J. Zhou, Finger typing driven triboelectric nanogenerator and its use for instantaneously lighting up LEDs, Nano Energy 2 (2013) 491–497.
[31] K. Xia, J. Fu, Z. Xu, Multiple-frequency high-output triboelectric nanogenerator based on a water balloon for all-weather water wave energy harvesting, Adv. Energy Mater. 10 (2020), 2000426.
[32] F.R. Fan, Z.Q. Tian, Z.L. Wang, Flexible triboelectric generator, Nano Energy 1 (2012) 328–334.
[33] K. Xia, Z. Zhu, H. Zhang, C. Du, Z. Xu, R. Wang, Painting a high-output triboelectric nanogenerator on paper for harvesting energy from human body motion, Nano Energy 50 (2018) 571–580.
[34] K. Xia, D. Wu, J. Fu, Z. Xu, A pulse controllable voltage source based on triboelectric nanogenerator, Nano Energy 77 (2020), 105112.
[35] K. Xia, D. Wu, J. Fu, N.A. Hoque, Y. Ye, Z. Xu, A high-output triboelectric nanogenerator based on nickel–copper bimetallic hydroxide nanowrinkles for self-powered wearable electronics, J. Mater. Chem. A 8 (2020) 25995–26003.
[36] J.C. Qian, J. He, S. Qian, J. Zhang, X.S. Niu, X.M. Fan, C. Wang, X.J. Hou, J.L. Mu, W.P. Geng, X.J. Chou, A nonmetallic stretchable nylon-modified high performance triboelectric nanogenerator for energy harvesting, Adv. Funct. Mater. 30 (2020), 1907414.
[37] L. Wang, W.A. Daoud, Highly flexible and transparent polyionic-skin triboelectric nanogenerator for biomechanical motion harvesting, Adv. Energy Mater. (2018), 1803183.
[38] Z. Wen, Y. Yang, N. Sun, G. Li, Y. Liu, C. Chen, J. Shi, L. Xie, H. Jiang, D. Bao, Q. Zhuo, X. Sun, A wrinkled PEDOT:PSS film based stretchable and transparent triboelectric nanogenerator for wearable energy harvesters and active motion sensors, Adv. Funct. Mater. 28 (2018), 1803684.
[39] K.K. Zhou, Y. Zhao, X.P. Sun, Z.Q. Yuan, G.Q. Zheng, K. Dai, L.W. Mi, C.F. Pan, C. T. Liu, C.Y. Shen, Ultra-stretchable triboelectric nanogenerator as high-sensitive and self-powered electronic skins for energy harvesting and tactile sensing, Nano Energy 70 (2020), 104546.
[40] J.P. Costanzo, R.E. Lee Jr., Cryoprotection by urea in a terrestrially hibernating frog, J. Exp. Biol. 208 (2005) 4079–4089.
[41] K.B. Storey, J. Bischof, B. Rubinsky, Cryomicroscopic analysis of freezing in liver of the freeze-tolerant wood frog, Am. J. Physiol. 263 (1992) R185–R194.
[42] X.P. Morelle, W.R. Illeperuma, K. Tian, R. Bai, Z. Suo, J.J. Vlassak, Highly stretchable and tough hydrogels below water freezing temperature, Adv. Mater. 30 (2018), e1801541.
[43] Y.J. Peng, M.H. Pi, X.L. Zhang, B. Yan, Y.S. Li, L.Y. Shi, R. Ran, High strength, antifreeze, and moisturizing conductive hydrogel for human-motion detection, Polymer 196 (2020), 122469.
[44] Y. Jian, B. Wu, X. Le, Y. Liang, Y. Zhang, D. Zhang, L. Zhang, W. Lu, J. Zhang, T. Chen, Antifreezing and stretchable organohydrogels as soft actuators, Research 2019 (2019), 2384347.
[45] Y.K. Jian, S. Handschuh-Wang, J.W. Zhang, W. Lu, X.C. Zhou, T. Chen, Biomimetic anti-freezing polymeric hydrogels: keeping soft-wet materials active in cold environments, Mater. Horiz. 8 (2021) 351–369.
[46] Q.F. Rong, W.W. Lei, J. Huang, M.J. Liu, Low temperature tolerant organohydrogel electrolytes for flexible solid-state supercapacitors, Adv. Energy Mater. 8 (2018), 1801967.
[47] X.T. Jin, L. Song, H.S. Yang, C.L. Dai, Y.K. Xiao, X.Q. Zhang, Y.Y. Han, C.C. Bai, B. Lu, Q.W. Liu, Y. Zhao, J.T. Zhang, Z.P. Zhang, L.T. Qu, Stretchable supercapacitor at −30 °C, Energy Environ. Sci. 14 (2021) 3075–3085.
[48] Q. Rong, W. Lei, L. Chen, Y. Yin, J. Zhou, M. Liu, Anti-freezing, conductive self-healing organohydrogels with stable strain-sensitivity at subzero temperatures, Angew. Chem. Int. Ed. 56 (2017) 14159–14163.
[49] Y. Xu, Q. Rong, T. Zhao, M. Liu, Anti-Freezing multiphase gel materials: bioinspired design strategies and applications, Giant 2 (2020), 100014.
[50] T. Pinarbasi, M. Sozbilir, N. Canpolat, Prospective chemistry teachers' misconceptions about colligative properties: boiling point elevation and freezing point depression, Chem. Educ. Res. Pract. 10 (2009) 273–280.
[51] F.C. Andrews, Colligative properties of simple solutions, Science 194 (1976) 567–571.
[52] T.X. Yu, L.S. Zhao, Q.A. Wang, Z.X. Cao, Glass transition behavior of ternary disaccharide-ethylene glycol-water solutions, Chem. Phys. Lett. 677 (2017) 172–177.
[53] X. Pu, M. Liu, X. Chen, J. Sun, C. Du, Y. Zhang, J. Zhai, W. Hu, Z.L. Wang, Ultrastretchable, transparent triboelectric nanogenerator as electronic skin for biomechanical energy harvesting and tactile sensing, Sci. Adv. 3 (2017), e1700015.
[54] T. Jin, Z. Sun, L. Li, Q. Zhang, M. Zhu, Z. Zhang, G. Yuan, T. Chen, Y. Tian, X. Hou, C. Lee, Triboelectric nanogenerator sensors for soft robotics aiming at digital twin applications, Nat. Commun. 11 (2020) 5381.
[55] W. Xu, L.B. Huang, M.C. Wong, L. Chen, G.X. Bai, J.H. Hao, Environmentally friendly hydrogel-based triboelectric nanogenerators for versatile energy harvesting and self-powered sensors, Adv. Energy Mater. 7 (2017), 1601529.
[56] K. Parida, G. Thangavel, G. Cai, X. Zhou, S. Park, J. Xiong, P.S. Lee, Extremely stretchable and self-healing conductor based on thermoplastic elastomer for all-three-dimensional printed triboelectric nanogenerator, Nat. Commun. 10 (2019) 2158.
[57] Y. Ren, J. Guo, Z. Liu, Z. Sun, Y. Wu, L. Liu, F. Yan, Ionic liquid-based click-ionogels, Sci. Adv. 5 (2019), eaax0648.
[58] H.L. Sun, Y. Zhao, S.L. Jiao, C.F. Wang, Y.P. Jia, K. Dai, G.Q. Zheng, C.T. Liu, P. B. Wan, C.Y. Shen, Environment tolerant conductive nanocomposite organohydrogels as flexible strain sensors and power sources for sustainable electronics, Adv. Funct. Mater. 31 (2021), 2101696.
[59] L.B. Huang, X.Y. Dai, Z.H. Sun, M.C. Wong, S.Y. Pang, J.C. Han, Q.Q. Zheng, C. H. Zhao, J. Kong, J.H. Hao, Environment-resisted flexible high performance triboelectric nanogenerators based on ultrafast self-healing non-drying conductive organohydrogel, Nano Energy 82 (2021), 105724.
[60] T. Jing, B. Xu, Y. Yang, M. Li, Y. Gao, Organogel electrode enables highly transparent and stretchable triboelectric nanogenerators of high power density for robust and reliable energy harvesting, Nano Energy 78 (2020), 105373.
[61] L. Sun, S. Chen, Y. Guo, J. Song, L. Zhang, L. Xiao, Q. Guan, Z. You, Ionogel-based, highly stretchable, transparent, durable triboelectric nanogenerators for energy harvesting and motion sensing over a wide temperature range, Nano Energy 63 (2019), 103847.
[62] Y. Hu, M. Zhang, C. Qin, X. Qian, L. Zhang, J. Zhou, A. Lu, Transparent, conductive cellulose hydrogel for flexible sensor and triboelectric nanogenerator at subzero temperature, Carbohydr. Polym. 265 (2021), 118078.
[63] D.Q. Bao, Z. Wen, J.H. Shi, L.J. Xie, H.X. Jiang, J.X. Jiang, Y.Q. Yang, W.Q. Liao, X. H. Sun, An anti-freezing hydrogel based stretchable triboelectric nanogenerator for biomechanical energy harvesting at subzero temperature, J. Mater. Chem. A 8 (2020) 13787–13794.
[64] Y. Wang, L.N. Zhang, A. Lu, Highly stretchable, transparent cellulose/PVA composite hydrogel for multiple sensing and triboelectric nanogenerators, J. Mater. Chem. A 8 (2020) 13935–13941.
[65] Z. Liu, Y. Wang, Y. Ren, G. Jin, C. Zhang, W. Chen, F. Yan, Poly(ionic liquid) hydrogel-based anti-freezing ionic skin for a soft robotic gripper, Mater. Horiz. 7 (2020) 919–927.